Dissipation of Mechanical Energy in Fused Silica Fibers

Andri M. Gretarsson* and Gregory M. Harry†
Department of Physics, Syracuse University, Syracuse, NY13244-1130

Abstract

To determine the dissipation induced by the surface of fused silica fibers, we measured the quality factor of fibers having various diameters. We measured a maximum quality factor of 21 million and extrapolated to obtain an intrinsic quality factor for fused silica of 30 million. Dissipation in the surface dominated at diameters less than about 1 mm. We developed a method for characterizing surface-induced dissipation that is independent of sample geometry or mode shape.

*Electronic mail: andri@phy.syr.edu

†Electronic mail: gharry@phy.syr.edu

I. INTRODUCTION

In experiments of sufficiently high sensitivity, fluctuations in the thermal energy of signal-band degrees of freedom can be an important source of noise. These fluctuations are due to coupling between the signal-band degrees of freedom of the detector and the thermal bath of other degrees of freedom. Since this coupling is also the cause of dissipation, one can relate the thermal noise in a detector to the dissipation of signal-band excitations. The relationship is quantified, for a wide class of couplings, by the Fluctuation-Dissipation Theorem:

$$x^2(f) = \frac{k_B T}{\pi^2 f^2} Re\left[\frac{1}{Z(f)}\right], \tag{1}$$

where $x(f)$ is the spectral density of the fluctuations, T is the temperature of the detector, and $Z^{-1}(f)$ is the admittance of detector excitations.[1,2] The real part of the admittance is proportional to the dissipation, so to minimize the thermal noise of a detector at a given temperature we must minimize its dissipation.

In mechanical experiments, such as gravitational wave detectors, the relevant thermally excited degrees of freedom are actual mechanical vibrations of detector components. The level at which such a detector is limited by thermal noise can therefore depend on the internal friction of the material from which the detector components are fabricated. The lower the dissipation in the material, the lower the thermal noise. Fused silica (synthetic amorphous SiO_2) has extremely low dissipation for audio frequency oscillations at room temperature. Therefore, fused silica is an excellent choice of material for the fabrication of critical components of a thermal noise limited detector, operating at room temperature in the audio frequency regime.[3]

Many authors have reported measurements of the dissipation in fused silica.[4–9] However, the measured quality factors, Q, are usually limited by dissipation mechanisms other than the intrinsic dissipation of the bulk material.[10–12] Particularly worrisome is the effect of a structurally defective and chemically impure surface, such as might result from normal handling, exposure to the atmosphere, or differential cooling during fabrication.[13] Although the current investigations are focused on fused silica, the condition of the surface is also a concern for other high-Q materials.[14]

To investigate the amount of dissipation induced by the surface, we measured the dissipation in fused silica fibers of varying diameters, and hence varying surface-to-volume ratios. In addition to providing information about the effect of the surface, our results may be extrapolated to give an approximate value for the dissipation in the bulk material.

II. THE EXPERIMENT

Our fibers were hand drawn in air, from Heraeus Co. "Suprasil 2"-brand fused silica rods, using a natural gas flame. The rods had diameters between 5 and 9 mm, and the fibers were drawn from the rods as supplied, with no additional surface preparation, either before or after drawing.

The dissipation in the fibers was measured at room temperature using the ringdown method.[15,10] Figure 1 shows the experimental setup. The fibers, hanging freely, were excited

with a comb capacitor providing an oscillating electric field with a large gradient.[16] Due to the dielectric properties of fused silica, an oscillating force is felt by the fiber. After a resonant mode was excited, the field was turned off, the capacitor grounded, and the fiber allowed to ring freely.

The displacement of the fiber as a function of time was measured by a split photodiode shadow sensor. The envelope of the displacement was extracted and fit to the functional form

$$x_0 e^{-\pi f_n \phi(f_n) t} + C, \tag{2}$$

where t is time, x_0 is the initial amplitude, C is the level of sensor and amplifier noise, and $\phi(f_n)$ is the loss angle at the resonance frequency f_n. (The quality factor of a resonance is equal to the reciprocal of the loss angle; $Q = \phi(f_n)^{-1}$.) In this experiment the dominant source of noise was sensor and amplifier noise. Equation 2 does not include a term describing seismic excitation of the fiber, which unlike sensor and amplifier noise, adds to the signal in quadrature.[17] At the frequencies of interest, seismic excitation of fiber resonant modes was not detectable above the sensor and amplifier noise, and including such a term in Eq. 2 did not measurably improve the quality of the fits.

Great care was taken to eliminate all extrinsic sources of dissipation, or "excess loss." In any measurement of fiber Q's, there are several sources of excess loss that must be considered: residual gas damping, rubbing at the clamp-fiber interface, recoil damping, and eddy-current damping.[10]

The damping due to residual gas molecules in the vacuum chamber is given by

$$\phi_{gas} = \frac{\bar{v}}{\pi f d} \frac{\rho_{gas}}{\rho_{fiber}}, \tag{3}$$

where d is the fiber diameter, f is the frequency of vibration, $\bar{v}$ is the average speed of the gas molecules, ρ_{gas} is the mass density of the gas, and ρ_{fiber} is the mass density of the fiber. Gas damping was made negligible by conducting our measurements at pressures around 10^{-6} torr. Taking typical values for the parameters, we estimate $\phi_{gas} \approx 10^{-9}$.

To eliminate rubbing at the clamp-fiber interface we ensured that the fiber oscillation did not induce elastic deformation of the fiber material in the clamp. This was achieved by drawing the fiber monolithically from a much thicker rod (i.e. leaving the fiber attached to the rod from which it was drawn), then clamping the rod in a collet as shown in Fig. 1.[18]

Recoil damping is due to coupling between the resonant modes of the fiber and low-Q resonances of the support structure. Resonant modes of the fiber having frequencies close to resonances of the supporting structure will be very strongly damped, while other modes will not be as strongly coupled and will have less recoil damping. The main diagnostic for recoil damping is therefore a strong frequency dependence of the Q.[12] In this experiment, recoil damping was minimized by isolating the fiber resonances from the support resonances by a structure analogous to a double pendulum. This also serves to isolate the fiber from seismic excitation at the frequencies of interest. Figure 2 shows the three different double pendulum type structures used in this experiment. The structures were monolithic to prevent interfacial rubbing, and in each case we measured the dissipation in the lowest fiber only. In the design of type 3, the lowest "fiber" is simply the undrawn rod, as supplied.

Eddy-current damping occurs when the oscillating fiber carries a charge, and the motion of the charges induces eddy currents in nearby conductors. Resistance in the conductors dissipates the mechanical energy stored in the currents, degrading the Q. The dissipation in any given fiber was not noticeably dependent on the arrangement of, or distance to, nearby conductors. We conclude that eddy-current damping was negligible in our measurements.

Finally, we note that our fibers were drawn from fused silica rather than fused quartz rods. Fused quartz is fabricated from naturally occurring SiO_2, while fused silica is made of synthetic SiO_2. Fused quartz has been measured to have intrinsic room temperature Q's of at most a few million.[4,17,19,20] These values are too low for our purposes and would obscure the dissipation induced by the surface layer.

Figure 3 shows the variations in Q measured with and without some of the precautions mentioned above. If the fiber is held directly in a clamp instead of being left attached to the rod from which it was drawn, friction due to rubbing in the clamp dominates. Without an isolation bob, recoil damping dominates and there is strong frequency dependence. Fibers clamped and hung by the rods from which they were drawn, and having a central isolation bob show the highest Q's, with much less frequency dependence. In these fibers, the difference between fused quartz and fused silica becomes apparent, with fused silica exhibiting substantially higher Q.

III. DISSIPATION VERSUS FREQUENCY FOR A TYPICAL FIBER

For each fiber, the dissipation was measured at a number of resonance frequencies. For fibers of the type 1 design, the resonance frequencies agree well with the resonance frequencies of a beam of circular cross section clamped at one end:

$$f_n = \begin{cases} \frac{\pi}{8}\sqrt{\frac{Yd^2}{\rho L^4}}(0.597)^2 & n = 1 \\ \frac{\pi}{8}\sqrt{\frac{Yd^2}{\rho L^4}}(n-\frac{1}{2})^2 & n \geq 2, \end{cases} \tag{4}$$

where Y is Young's modulus, d is the fiber diameter, L is the fiber length, ρ is the mass per unit volume, and $n = 1, 2 \ldots$ is the mode number.[21] Figure 4 shows the agreement between the measured and predicted resonance frequencies for a typical fiber of type 1. The mode frequencies may be used to calculate the diameter of the fiber, and we find good agreement with the average diameter measured using a micrometer. Similarly, for the fibers of type 3, the resonance frequencies agree with those of a free beam of circular cross section. As expected, the resonance frequencies of the fiber of type 2 are not well modeled by either a free or a clamped beam. This is due to the large diameter of the excited fiber relative to the first (lowest) isolation bob which takes some part in the motion. Because of this, the fiber of type 2 was made with an extra isolation bob.

Figure 5 shows the dissipation versus frequency for the fiber whose resonance frequencies are shown in Fig 4. The graph shows a loss peak around 100 Hz which is due to thermoelastic damping.[22] Thermoelastic damping is given by

$$\phi_{therm} = \frac{Y\alpha^2 T_0}{C}\frac{\sigma f}{1+\sigma^2 f^2}, \tag{5}$$

where Y is Young's modulus, α is the thermal expansion coefficient, T_0 is the fiber temperature (absolute scale), C is the heat capacity per unit volume, and f is the frequency of vibrations. The constant σ is

$$\sigma = \frac{2\pi}{13.55}\frac{Cd^2}{\kappa},$$

where d is the fiber diameter and κ is the thermal conductivity. We found good agreement between the average measured diameter and the diameter calculated from the position of the thermoelastic damping peak.

As can be seen from the graph, the dissipation is not purely thermoelastic and can be modeled by the form

$$\phi(f) = \phi_{therm}(f) + \phi_c, \tag{6}$$

where $\phi_{therm}(f)$ is thermoelastic damping and ϕ_c is a frequency-independent damping term. The dissipation in most of the fibers is in good overall agreement with the form of Eq. 6. (Several fibers have a small number of modes showing anomalously high dissipation. This indicates an undiagnosed source of dissipation affecting these modes.)

The appearance of a frequency-independent loss angle ϕ_c suggests the presence of a dissipation source whose microscopic components have a wide range of activation energies.[23] Dissipation in the bulk material is likely to be of this type. However, a frequency-independent term might also arise from defects or impurities in the surface layer, or possibly from other sources.

One way of obtaining further information as to the source of ϕ_c is to measure its dependence on the fiber diameter. In this way it is possible to distinguish between dissipation occurring in the bulk volume of the fiber and dissipation occurring in the surface layer.

IV. MODEL OF DIAMETER DEPENDENCE

The constant loss angle ϕ_c is modeled as consisting of two parts, one due to dissipation in the bulk and one due to dissipation in the surface layer:

$$\phi_c = (\Delta E_{bulk} + \Delta E_{surf})/E, \tag{7}$$

where ΔE_{bulk} is the energy lost per cycle in the bulk material, ΔE_{surf} is the energy lost per cycle in the surface layer, and E is the total energy stored in the oscillating fiber.

If we make the rather general assumption that ΔE_{surf} is proportional to the surface area S while ΔE_{bulk} is proportional to the volume V, we may write

$$\frac{\Delta E_{surf}}{\Delta E_{bulk}} \propto \frac{S}{V}. \tag{8}$$

The coefficient of proportionality depends on the ratio of the loss angle of the surface layer to the loss angle of the bulk material. It also depends on the ratio of energy stored in the surface layer to energy stored in the bulk. Some complication arises because both the loss angle of the surface layer and the density of energy stored in the surface layer are functions of depth. While we can normally calculate the energy density from the strain profile of the

mode shape, we know little about dissipation in the surface layer. Since we are interested in characterizing the dissipation in the surface independently of the mode of oscillation or sample geometry, we write the coefficient of proportionality as a product of two factors

$$\frac{\Delta E_{surf}}{\Delta E_{bulk}} = \mu \frac{d_s}{V/S}. \tag{9}$$

The geometrical factor μ depends only on the geometry of the sample and on the mode of oscillation, while the "dissipation depth" d_s depends only on the strength of dissipation in the surface layer relative to the bulk. The appropriate expressions for μ and d_s are calculated in the Appendix. When the Young's modulus of the surface layer is the same as that of the bulk, we have

$$d_s = \frac{1}{\phi_{bulk}} \int_0^h \phi(n) dn, \tag{10}$$

where n is a coordinate measuring the distance inward from the surface, $\phi_{bulk} \equiv \Delta E_{bulk}/E_{bulk}$ is the loss angle of the bulk material, $\phi(n)$ is the loss angle of the surface layer as a function of depth, and h is the thickness of the surface. For our fibers, having circular cross section and oscillating in transverse modes, we have $\mu = 2$.

For samples with simple geometries, μ is of order unity and the volume-to-surface ratio has the same order of magnitude as the minimum thickness of the sample. When the dissipation depth is small compared to the minimum thickness of the sample, the effect of the surface on the dissipation is also small. When the dissipation depth is greater than or on the order of the minimum thickness of the sample, dissipation in the surface is likely to dominate.

Since $\phi(n)$ is seldom known explicitly, a measurement of the dissipation depth provides a convenient way of comparing the surface condition of different samples made of the same material. Since $E \approx E_{bulk}$ we may rewrite Eq. 7 in terms of the dissipation depth,

$$\phi_c = \phi_{bulk}(1 + \mu \frac{d_s}{V/S}). \tag{11}$$

In our case $V/S = d/4$, and the theory predicts

$$\phi_c = \phi_{bulk}(1 + 8\frac{d_s}{d}). \tag{12}$$

Equation 12 is the model to which we shall compare our data on dissipation versus fiber diameter.

V. DISSIPATION VERSUS DIAMETER

For all of the fibers, the constant loss angle ϕ_c was measured with the surface condition "as drawn". The surface of fibers drawn in a flame is largely free from microcracks[24,25] and we tried to avoid damaging this surface. Although care was taken during transport and during installation in the apparatus, some of the fibers did get lightly knocked against

aluminum or glass components. This represents the only physical contact with the fiber surface.

Measurements of ϕ_c were made in the following way. Since $\phi(f) \rightarrow \phi_c$ far from the thermoelastic damping peak, a measurement of the total loss angle ϕ at a frequency where thermoelastic damping is known to be negligible, constitutes a direct measurement of ϕ_c. In each case ϕ_c was taken as the lowest measured value of the loss angle for a particular fiber. In most cases, measurements of ϕ could be taken at a sufficiently large range of frequencies so that those modes exhibiting the lowest dissipation gave a good approximation to the ϕ_c asymptote. The three thickest fibers however, posed some problems. We were only able to excite two or three modes in each, and no direct verification could be made of the existence of a ϕ_c asymptote. In addition, the dissipation in these fibers is very small, and correspondingly more sensitive to excess loss. Table I lists the Q's measured for the three thickest fibers. While Fiber G exhibits constant Q's, the Q's of Fiber J and Fiber K are quite frequency dependent. This is particularly striking for the split-frequency, third resonance mode of Fiber K, where the Q changes by a factor of 3 within 4 Hz. The source of this excess loss is undiagnosed.

Figure 6 shows ϕ_c versus diameter for the 10 fibers measured. Systematic errors are likely to be far larger than the uncertainty shown (which represents the repeatability). The main source of systematic error is the upward bias of the measured dissipation due to undiagnosed sources of excess loss. We fit the data to Eq. 12 and have tried to minimize the error induced by undiagnosed excess loss by including in the fit only those fibers whose graphs of dissipation versus resonance frequency do not have points deviating significantly from the form predicted by Eq. 6. (For example, the fiber whose dissipation versus frequency data is shown in Fig. 5 satisfies this criterion well.) The fit determines d_s and ϕ_{bulk}, which have the values

$$d_s = 180 \pm 20 \ \mu\text{m}, \tag{13}$$

$$\phi_{bulk} = 3.3 \pm 0.3 \times 10^{-8}. \tag{14}$$

The relationship between d_s and other measures of surface condition (fiber strength, surface roughness, impurities, etc.) is an interesting and open question. Further research is required to understand the dependence on surface preparation methods, storage times, manufacturing and handling, etc. The above value for ϕ_{bulk} is consistent with the lowest dissipation measured in fused silica.[5,8] A quality factor of approximately 3×10^7 has been seen in hemispherical resonators of surface-treated, Russian brand KS4V fused silica at 3.7 kHz.[26]

With knowledge of the dissipation depth, we can use Eq. 9, to calculate the fiber diameter, d_{eq}, at which surface-induced dissipation becomes equal in importance to bulk-induced dissipation:

$$d_{eq} = 8d_s \approx 1300 \ \mu\text{m}.$$

In order to obtain an estimate for the average loss angle in the surface layer, we model the surface layer as a homogeneous shell of thickness h having a depth-independent loss angle, $\phi(\vec{r}) \equiv \phi_{surf}$. Equation 10 gives

$$d_s = h\frac{\phi_{surf}}{\phi_{bulk}}. \tag{15}$$

The literature suggests several mechanisms for chemical surface damage penetrating to a depth of order 1 μm.[27] Taking $h = 1$ μm and using the values given by Eqs. 13 and 14 we obtain

$$\phi_{surf} \approx 10^{-5}. \tag{16}$$

ACKNOWLEDGEMENTS

We would like to thank Peter Saulson for advice, suggestions, support, and careful reading of the manuscript. We also thank William Startin and Steven Penn for useful discussions and reading the manuscript. Thanks to Yinglei Huang for teaching us the basics of fiber measurements and to Mark Beilby for helpful discussions. Additional thanks are due to Vinod Balachandran for contributing his time in the lab during the summer of 1998, and to John Schiller who is extending this work by performing surface treatments on fused silica fibers. We thank James Hough and the anonymous referee for pointing out the correct way of including seismic noise in the description of a ringdown envelope. We would especially like to thank the glassblower to Syracuse University, John Chabot, who drew all the fibers used in these measurements. This work was supported by Syracuse University and by National Science Foundation grant PHY-9602157.

APPENDIX: FORM OF THE GEOMETRICAL FACTOR AND THE DISSIPATION DEPTH

It is possible (in a continuum approximation) to define a point loss angle,

$$\phi(\vec{r}) \equiv \Delta\rho_E(\vec{r})/\rho_E(\vec{r}), \tag{A1}$$

where $\vec{r}$ represents the location within the sample, $\rho_E(\vec{r})$ is the energy density stored at $\vec{r}$, and $\Delta\rho_E(\vec{r})$ is the negative change in $\rho_E(\vec{r})$ per cycle.

The bulk may then be defined as the region of points within the sample where $\phi(\vec{r})$ is constant. For the purposes of our model, we assume that there exists a surface layer of maximum thickness h where $\phi(\vec{r})$ varies, while elsewhere in the sample $\phi(\vec{r})$ has the constant value ϕ_{bulk}.

Recalling

$$\rho_E(\vec{r}) = \frac{1}{2} Y(\vec{r}) \epsilon^2(\vec{r}) \tag{A2}$$

where $Y(\vec{r})$ is the Young's modulus and $\epsilon(\vec{r})$ the strain amplitude, we can write

$$\Delta E_{surf} = \frac{1}{2} \int_{\mathcal{SL}} \phi(\vec{r}) Y(\vec{r}) \epsilon^2(\vec{r})\, d^3r \tag{A3}$$

where $\mathcal{SL}$ is the region constituting the surface layer. If we make the assumption that $\phi(\vec{r})$ and $Y(\vec{r})$ may be treated as functions of depth alone, we can write

$$\Delta E_{surf} = \frac{1}{2}\int_0^h \phi(n)Y(n)\left\{\int_{\mathcal{S}(n)} \epsilon^2(\vec{r})d^2r\right\} dn, \tag{A4}$$

where n measures the distance in from the surface and $\mathcal{S}(n)$ is a surface of integration at depth n, parallel to the actual surface of the sample. For the bulk we have

$$\Delta E_{bulk} = \frac{1}{2}\phi_{bulk}Y_{bulk}\int_{\mathcal{V}} \epsilon^2(\vec{r})d^3r \tag{A5}$$

where $\mathcal{V}$ is the region of the bulk and Y_{bulk} is Young's modulus of the bulk.

We now make the assumption that h is sufficiently small that

$$\epsilon(\vec{r} \in \mathcal{SL}) \approx \epsilon(\vec{r} \in \mathcal{S}), \tag{A6}$$

where $\mathcal{S} = \mathcal{S}(0)$ is the actual surface of the sample. Using Eqs. A4–A6 we can write

$$\frac{\Delta E_{surf}}{\Delta E_{bulk}} = \mu\frac{d_s}{V/S}, \tag{A7}$$

where V is the volume of the sample, S is its surface area, and μ and d_s are assigned the values

$$\mu = \frac{V}{S}\frac{\int_{\mathcal{S}} \epsilon^2(\vec{r})d^2r}{\int_{\mathcal{V}} \epsilon^2(\vec{r})d^3r}, \tag{A8}$$

$$d_s = \frac{1}{\phi_{bulk}Y_{bulk}}\int_0^h \phi(n)Y(n)dn. \tag{A9}$$

The geometrical factor μ is a dimensionless constant which depends only on the sample geometry and on the class of resonances excited. The dissipation depth d_s has the dimensions of length and provides a direct measure of the total dissipation induced by the surface layer (normalized to the dissipation in the bulk). In uncoated samples, the dissipation depth provides a measure of the physical and chemical damage suffered by the surface of the sample.

For a transversely oscillating fiber of circular cross section, the strain amplitude is given, in cylindrical coordinates, by

$$\epsilon(\vec{r}) = \frac{\partial^2 u(z)}{\partial z^2}\, r\cos\theta, \tag{A10}$$

where $u(z)$ is the displacement amplitude of the fiber from equilibrium. Using Eq. A8 we immediately have

$$\mu = 2. \tag{A11}$$

REFERENCES

[1] H. B. Callen and T. A. Welton, Phys. Rev. **83** 35 (1951); H. B. Callen and R. F. Greene, *ibid.* **86** 703 (1952).

[2] P. R. Saulson, Phys. Rev. D **42** 2437 (1990).

[3] V. B. Braginsky, V. P. Mitrofanov, and V. I. Panov, *Systems with Small Dissipation*, English Translation by Erast Gliner, The University of Chicago Press, Chicago, 1985.

[4] D. B. Fraser, J. Appl. Phys. **39**, 5868 (1968); **41**, 6 (1970).

[5] W. J. Startin, M. A. Beilby, and P. R. Saulson, Rev. Sci. Instr. **69** 3681 (1998)

[6] A. D. Gillespie, PhD. thesis (California Institute of Technology, 1995) Unpublished.

[7] M. N. Danchevskaya, B. S. Lunin, I. V. Batov, V. N. Smirnov, A. N. Tselbrovsky, G. P. Panasyuk, and V. B. Lazarev, Proceedings of the X$^{\text{th}}$ National Scientific and Technical Conference–Glass and Fine Ceramics–Summaries, Vol. 1, Glass; Varna Bulgaria, October 18-20, 1990, pp. 197-198.

[8] M. N. Danchevskaya, B.S. Lunin, and I.V. Batov, VII$^{\text{th}}$ All-Union Scientific-Technical Conference on Fused Silica, Reports, St. Petersburg, Nov. 19-20, 1991. (Transl. by L. Espovitch for Delco Systems Operations.)

[9] E. J. Loper, D. D. Lynch, and K. M. Stevenson, IEEE PLANS (Position Location and Navigation Symposium) Record, Caesar's Palace, Las Vegas, Nevada, November 4-7, 1986, pp. 61-64, Table 2.

[10] Y. L. Huang and P. R. Saulson, Rev. Sci. Instr. **69** 544 (1998)

[11] V. B. Braginsky, V. P. Mitrofanov, K. V. Tokmakov, Physics Doklady **40** 564 (1995), Transl. from Doklady Akademii Nauk, **345** 324 (1995)

[12] J.E. Logan, N. A. Robertson, J. Hough, Phys. Lett. A **170** 352 (1992).

[13] B.S. Lunin, S. N. Torbin, M. N. Danchevskaya, and I. V. Batov, Mos. Univ. Chem. Bull., **35** 24 (1994)

[14] L. Ju, D.G. Blair, M. Taniwaki, and R. Andrew, Phys. Lett. A **254** 239 (1999).

[15] J. Kovalik and P. R. Saulson, Rev. Sci. Instr. **64** 2942 (1993).

[16] A. Cadez and A. Abramovici, J. Phys E: Sci. Instr. **21** 453 (1988).

[17] S. Rowan, R. Hutchins, A. McLaren, N. A. Robertson, S. M. Twyford, and J. Hough, Phys. Lett. A, **227** 153 (1997).

[18] T. J. Quinn, C.C. Speake, W. Tew, R. S. Davis, and L. M. Brown, Phys. Lett. A, **197** 197 (1995).

[19] S. Rowan, S. M. Twyford, J. Hough, D.-H. Gwo, and R. Route, Phys. Lett. A, **246** 471 (1998).

[20] G. Cagnoli, Presentation at LIGO Scientific Collaboration Meeting, Gainesville, Florida, March 1999.

[21] P. M. Morse, *Vibration and Sound*. McGraw-Hill, 1948.

[22] C. Zener, Phys. Rev. **52** 230 (1937).

[23] F. K. du Pré, Phys. Rev. **78** 615 (1950).

[24] R. H. Doremus, *Glass Science*, pp. 284-285, John Wiley & Sons, New York, 1973.

[25] D.R. Uhlman and N.J. Kreidl ed., *Elasticity and Strength in Glasses*, Academic Press, New York, 1980.

[26] B. S. Lunin, Chemistry Department, Moscow State University, Private communication, May 4, 1997.

[27] R. H. Doremus, in *Treatise on Material Science and Technology*, Vol. 17, Academic Press, New York, 1979.

FIGURES

FIG. 1. Schematic diagram of the experimental setup. The signal from the split photodiode shadow sensor is fed through a differential amplifier, bandpass filter, a lock-in amplifier and computer data acquisition system.

FIG. 2. Three different designs for fiber isolation structures. In each case, only the dissipation in the lowest section was measured. In total, ten fibers were measured. Seven were of type 1, having diameters less than or equal to about 1050 μm, one was of type 2, having diameter of about 3500 μm, and two were of type 3, having diameters of about 4890 μm and 5930 μm.

FIG. 3. The effect of isolation techniques. The left-hand graph shows the results for three natural fused quartz fibers having diameters between 350 and 500 μm. The crosses indicate a fiber of type 1 (see Fig. 2) clamped in a collet by the rod from which it was drawn. The circles indicate a similar fiber clamped in a collet by the rod from which it was drawn, but lacking an isolation bob. The triangles indicate a fiber detached from the rod from which it was drawn, lacking an isolation bob, and clamped between two plates. The right-hand graph shows the results for a single fused silica fiber of type 1, having diameter approximately 400 μm. The crosses represent the fiber clamped in a collet by the rod from which it was drawn. The circles represent the same fiber, in the same collet, but clamped and hung from the isolation bob.

FIG. 4. Fit of theoretical cantilever beam resonance frequencies to the resonance frequencies of a typical fiber of type 1. The data shown is from a fiber of length 13 ± 1 cm and diameter 120 ± 20 μm. (The relatively large uncertainties are due to the taper where the fiber exits the central bob.) The crosses are the measured values and the solid line is a fit of the measured values to Eq. 4.

FIG. 5. Measured ϕ vs. resonance frequency for a typical fiber of type 1. The circled bars represent the measured dissipation and uncertainty. The solid line represents the theoretical thermoelastic plus constant damping and is a fit of the measured values to Eq. 6. The dashed line is the thermoelastic term from the fit.

FIG. 6. Measured ϕ_c vs. average measured fiber diameter. The circled points represent fibers whose dissipation vs. frequency graph follows Eq. 6 without anomalous points. The uncertainty in ϕ shown is the approximate repeatability (5%). The uncertainty shown in the average measured diameter is an estimate for the uncertainty induced by the fiber taper, where it exits the rod from which it was drawn. The solid line shows a least squares fit of Eq. 12 to the circled points. The diameter of the thinnest fiber was not measured directly but obtained from the position of the thermoelastic damping peak.

TABLES

TABLE I. Quality factors exhibited by the the three thickest fibers. Repeated measurements typically vary by about 5%; this is larger than the measurement uncertainty. The large uncertainty in the average measured diameter is due to the taper at the upper end of the fiber.

Table I

Sample	Avg. diameter (μm)	Mode number	f (Hz)	Q
Fiber G[a]	3500 ± 250	2	732.0 ± 0.1	2.1×10^7
		3	1582.5 ± 0.1	2.1×10^7
Fiber J[b]	4885 ± 120	2[c]	2157.3 ± 0.1	1.0×10^7
		2[c]	2167.3 ± 0.1	0.41×10^7
Fiber K[b]	5934 ± 70	3[c]	1725 ± 0.5	0.68×10^7
		3[c]	1729 ± 0.5	2.0×10^7
		4	3364.0 ± 0.1	0.35×10^7

[a]Type 2.
[b]Type 3.
[c]Since fiber cross sections are not perfectly circular, mode frequencies are split.

Figure 1, Gretarsson et al., Rev. Sci. Instr..

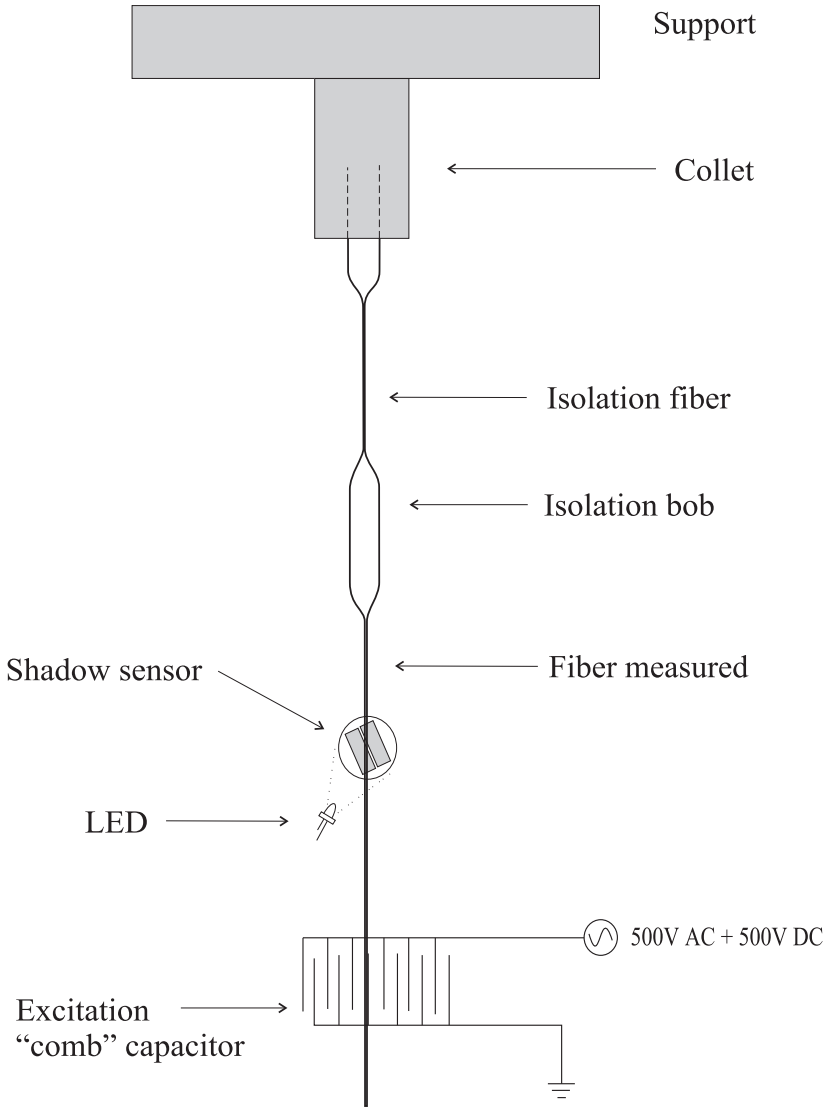

Figure 2, Gretarsson et al., Rev. Sci. Instr..

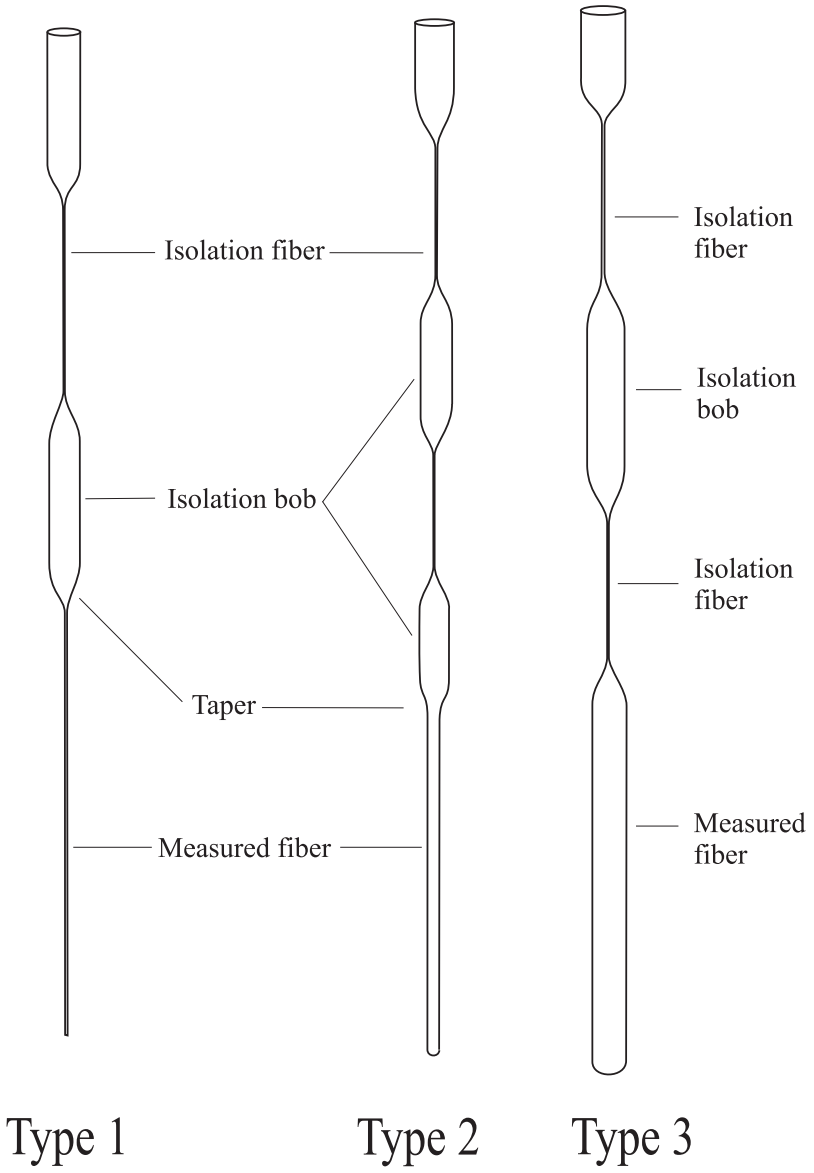

Figure 3, Gretarsson et al., Rev. Sci. Instr.

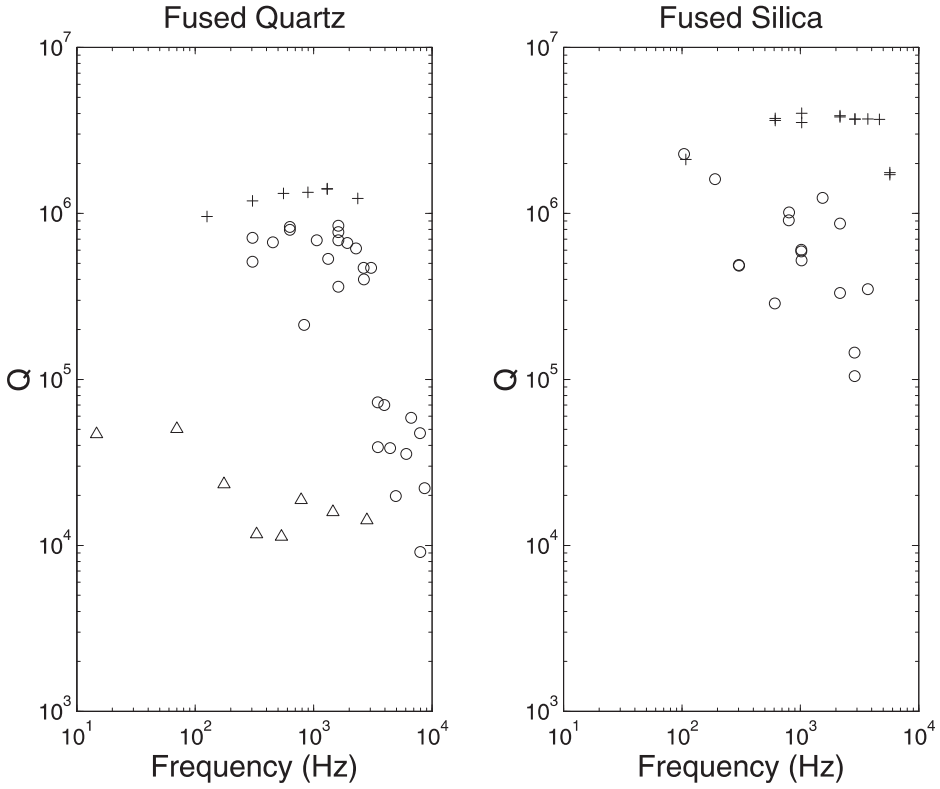

Figure 4, Gretarsson et al., Rev. Sci. Instr.

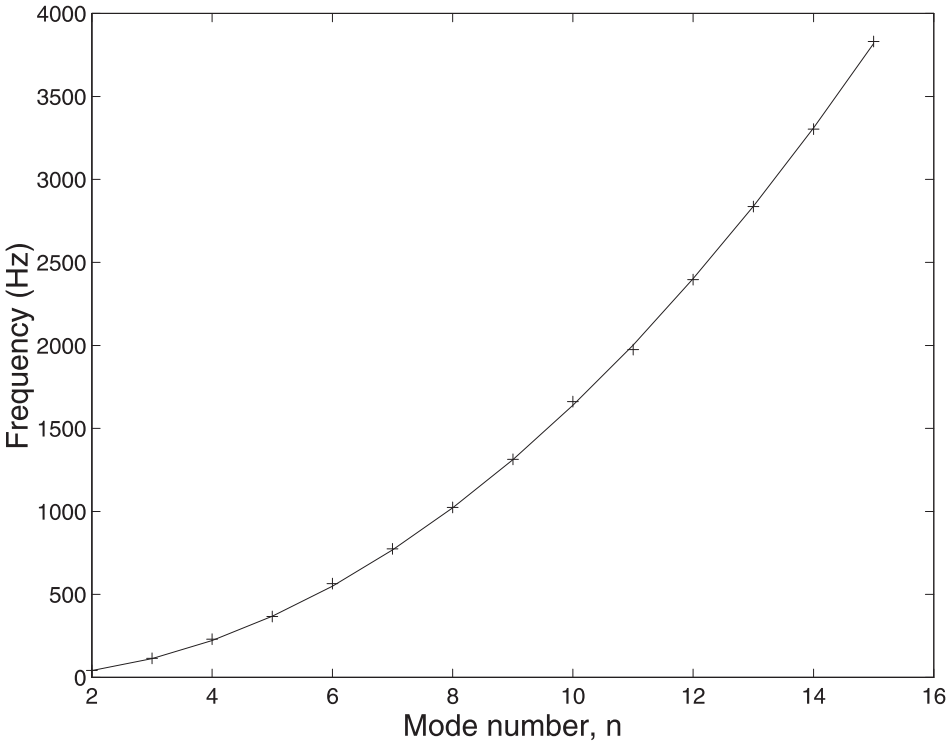

Figure 5, Gretarsson et al., Rev. Sci. Instr.

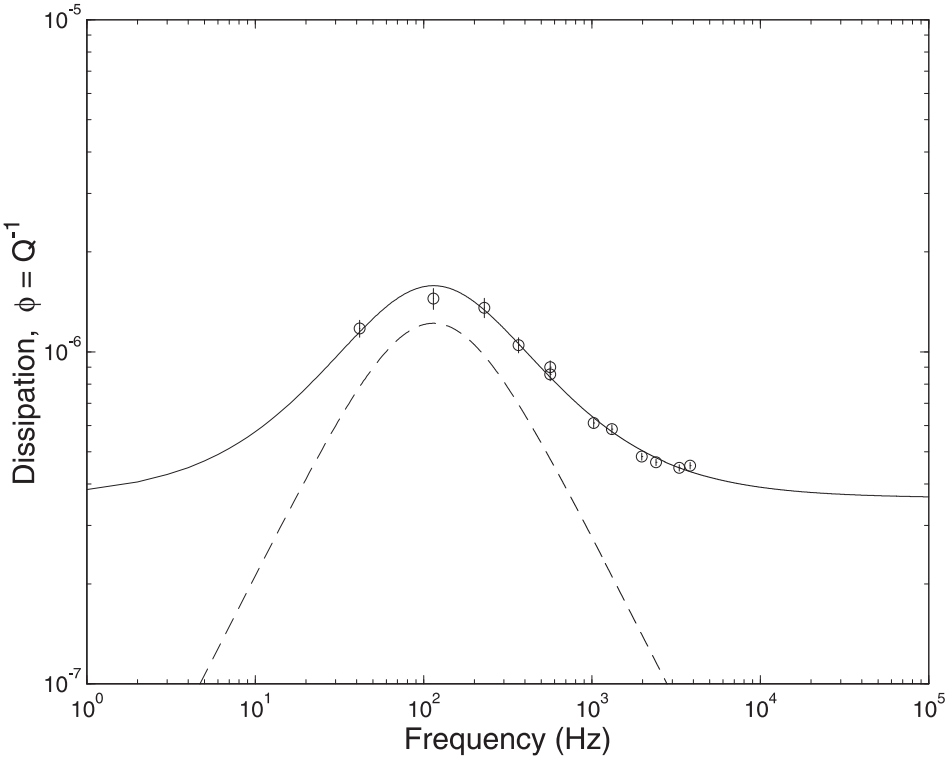

Figure 6, Gretarsson et al., Rev. Sci. Instr.